Journal Majelis Paspama
Volume 4 Number 02, 2026 (No. 243- 254)
E.SSN 2987-1379 (Online)

Design and Development of Hydrothermal Carbonization Reactor

[1]Calistus Princewill Odeh, [2]Orobosa Kingsley Osasuwa, [3]Augustine Uzodimma Madumere, [4]Sunday Chimezie Anyaora
Nnamdi Azikiwe University, Awka, Anambra State, Nigeria.
Email: cp.odeh@unizik.edu.ng

Article Info

Corresponding Author:
Calistus Princewill Odeh
E-mail: cp.odeh@unizik.edu.ng

ABSTRACT

This project presents the design, development, and evaluation of a hydrothermal carbonization (HTC) reactor for the conversion of biomass into carbon-rich hydrochar. The reactor was designed to operate under subcritical water conditions with controlled temperature and voltage inputs. Experimental tests were conducted at three voltage levels (185V, 210V, and 220V) and target operating temperatures of 180°C, 200°C, and 220°C. The results showed that heating rate and energy efficiency were directly influenced by voltage level. At higher voltages, the reactor attained the set temperatures in shorter times, with 220V achieving 220°C in 37 minutes compared to 44 minutes at 185V. The evaluation confirmed a linear correlation between temperature and time for all test conditions. The developed reactor demonstrates the potential for efficient thermal processing of wet biomass without prior drying, offering a sustainable pathway for waste-to-energy conversion. The study provides a foundation for further optimization of HTC reactor designs to enhance efficiency and scalability for industrial applications.

Keywords: Hydrothermal carbonization, Biomass, Reactor Design, Hydrochar, Temperature, Heating Rate, Energy Efficiency

INTRODUCTION

Global energy demand and climate concerns have driven research into renewable and low carbon energy technologies. The International Energy Agency (IEA) projects a significant rise in global energy consumption (e.g., 22.7 Gtoe by 2040), mainly to meet the needs of population and economic growth. At the same time, international agreements such as the COP21 Paris Accord aim to limit global warming to 1.5–2.0 °C, requiring a sharp reduction in greenhouse gas emissions and a transition away from fossil fuels. These pressures have spurred interest in converting biomass and waste into energy, thereby addressing both renewable energy needs and waste management problems (Sharma et al. 2020).

In Nigeria and many developing countries, energy deficits and poor waste management compound these global challenges. Umar et al. (2024) note that Nigeria faces an energy deficit alongside growing municipal and agricultural waste streams. They argue that "waste-to-energy" (WtE) technologies offer a sustainable solution to these coupled challenges. For example, Umar et al. estimate that converting municipal and agricultural wastes to energy could generate on the order of 10^1–10^2 terawatt-hours per year in Nigeria. However, realizing this potential requires overcoming technical, economic, and policy barriers (e.g., regulatory frameworks, investment, infrastructure). In particular, many abundant waste materials in Nigeria (e.g. agricultural residues, organic municipal waste) remain unutilized or inefficiently used, highlighting the need for new treatment and conversion technologies.

Biomass is abundant in Nigeria. Obi et al. (2023) report that Nigeria produces on the order of 10^8 tonnes of biomass per year (roughly 144 million tonnes annually). Most rural households rely on raw biomass (wood, charcoal, animal dung, crop residues) for cooking and heating, which poses health and environmental problems. Obi et al. emphasize that processing this biomass into cleaner fuels (such as briquettes, pellets, or hydrochars) could help diversify energy supply, reduce dependence on imported fossil fuels, and improve energy security. Despite its huge biomass endowment, Nigeria lacks sufficient infrastructure for clean biomass utilization. For example, only small-scale research has been done on densified fuels (briquettes, pellets) and gasification, and waste collection systems are weak

One underutilized biomass in West Africa is the African fan palm (Borassus aethiopum), also known as palmyra palm. This perennial tree produces edible fruit and large seeds ("fan palm nuts") that are often wasted or used for low-value applications (e.g., animal feed). The fibrous husks and residues from African fan palm operations could be a promising feedstock for energy conversion. To our knowledge, little work has been done on converting African fan palm biomass into fuel, especially using advanced thermochemical processes. However, similar palm-derived wastes (like oil palm empty fruit bunches and shells) have been explored elsewhere for bioenergy. For example, Suemanotham et al. (2022) used palm oil empty fruit bunches in a hydrothermal carbonization process to make biochar solid fuel. This suggests that palm wastes with high moisture content can be upgraded via thermochemical methods.

Hydrothermal carbonization (HTC) has recently emerged as a promising technology for converting wet biomass into carbon-rich fuels and materials. In HTC, biomass is treated in hot, pressurized water (typically 180–250 °C, autogenous pressure) for a period of time. This "wet pyrolysis" process hydrolyzes, dehydrates, and aromatizes the biomass into a hydrochar a coal-like solid that is dry, hydrophobic, and has a calorific value similar to lignite coal. Importantly, HTC can handle very wet feedstocks (30–90% moisture) without the need for costly drying, making it attractive for agricultural and waste biomass. As Reza et al. (2014) note, HTC effectively mimics nature's coalification under laboratory conditions, yielding a stable solid fuel and extracting nutrients or chemicals from the process water. The hydrochar product can serve as a solid biofuel or as a precursor for activated carbon and soil amendments, while the aqueous byproducts may be treated or valorized further. Because of these advantages, HTC has been applied to a wide range of wastes (food waste, sewage sludge, manure, etc.).

Existing studies illustrate the potential of HTC. For example, Wang et al. (2018) provide a comprehensive review of HTC process parameters and products. They highlight that HTC produces "energy and chemicals without pre-drying", and that the resulting hydrochar can replace coal or be used in environmental applications. Similarly, Ho et al. (2024) review the challenges of scaling HTC technology. They emphasize that HTC can convert diverse wet wastes to valuable products (biochar, bio-oil, etc.), but upscaling from laboratory to industrial scale requires careful reactor design, process control, and integration with other waste treatments. Pilot projects (e.g., Zaccariello et al., 2022) have begun to design bench- and pilot-scale HTC reactors to process biosolids or municipal waste, but each case demands specific engineering solutions. Although HTC is promising globally, its application to Nigerian biomass has been limited. Few studies have investigated HTC for local feedstocks in Nigerian conditions. The lack of proven HTC reactors adapted to Nigeria's context represents a technological gap. Designing a hydrothermal reactor requires addressing high pressures and temperatures, material selection, safety controls, and heating/cooling systems. Bench-scale HTC reactors typically use stainless-steel autoclaves with electrical heaters and instrumentation (thermocouples, pressure sensors). For example, Merzari et al. (2018) describe a 2-liter AISI-316 stainless steel batch reactor built to operate at up to 300 °C and 140 bar, heated by four 1-kW electrical resistors and instrumented with four internal thermocouples. This reactor included safety features (rupture disk, cold trap, pressure transducers) to ensure safe operation. Such designs demonstrate the complexity involved

In summary, the global energy and climate context points to the need for sustainable waste-to-energy solutions, especially in emerging economies like Nigeria. Nigeria has abundant biomass (including palm wastes) and a pressing waste and energy problem, but lacks pilot-scale facilities for advanced conversion like HTC. Hydrothermal carbonization is a well-established thermochemical process for wet biomass, yet the design of a dedicated HTC reactor for Nigerian feedstocks (e.g. African fan palm nut) remains an open challenge. Addressing this gap could enable local production of renewable solid fuels, improve waste management, and contribute to energy security and environmental goals.

METHODS

The development of the reactor was done by carrying out the graphic and mathematical design of the reactor. The design was simulated to ensure safe operations. The fabrication was done using selected materials according to the design specifications.

Graphic Design

The HTC reactor, consisting of multiple components including the supporting frame, reactor housing, reaction chamber, reactor gas tank, and electrical elements, was modelled using SolidWorks 2020. Each component was initially created as individual parts, which were subsequently assembled through mating operations. Materials and colours were selected from SolidWorks' extensive library and applied to the respective parts. The graphical outputs are presented in the following chapter.

Mathematical Design

Mathematical design calculations were performed to determine key parameters that guide material selection for reactor fabrication, ensuring safe and efficient operation.

Volume and Height of the Reaction Chamber

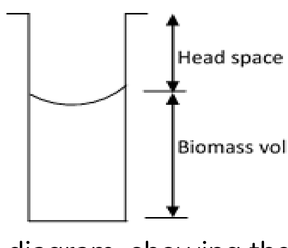

Figure 1: Schematic diagram, showing the volume of the reactor

From the design consideration, the volume of wet biomass (V_{wb}) was considered, hence the volume (V_r) and height (h_r) of the reaction chamber, considering 30% head space as seen in figure 3, will be given by equation (1) and (2) respectively as;

$$V_r = V_{wb} + 0.3\ (V_{wb}) \quad (1)$$

$$\mathrm{Vr} = \pi \left(\frac{d_r}{2}\right)^2 h_r \quad (2)$$

Where d_r is the diameter of the reaction chamber. (Ezenwa at al, 2023)

Reaction Chamber Wall Thickness

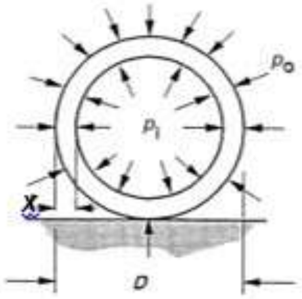

Figure 2: Schematic diagram, showing the cross section of the reaction chamber

Considering figure 4, P_i is the internal pressure developed within the reaction chamber, P_o is the atmospheric pressure acting on the surface, while d_r and x is the diameter and the thickness of the reaction chamber. To calculate the wall thickness of the reaction chamber, the type of stainless steel to be used is considered, in order to determine the thickness that will withstand the maximum working pressure and temperature. This was done using equation (3)

$$\sigma_h = (P_i - P_0)\frac{d_r}{2x} \times f_s \quad \text{(Bai et al, 2014)} \tag{3}$$

Where σ_h is the hoop stress, and it's been replaced with ultimate tensile strength during theoretical calculations (Reddy, 2005), and f_s is the factor of safety.

Heating Capacity

The wattage of the heating element to obtain the maximum heating rate is given;

$$E = \frac{mC_{p\Delta T}}{t} \tag{4}$$

Where E is the Wattage (watt) of the heating element,

Cp is the specific heat of the reactor material obtained from ASTM metal table chart,

ΔT is change in temperature between the desired maximum temperature (T_1) and the temperature of the environment (T_2), given by the expression;

$$\Delta T = (T_1 - T_2) \tag{5}$$

t is the required time to raise the temperature, and m is the mass of the reaction chamber material to be heated up, given by;

$$\rho = \frac{m}{V} \tag{6}$$

Where ρ is the density of the reactor material obtained from ASTM metal table chart, and v is the volume of the reaction chamber material used for the required volume, and it's given by;

$$V = (2\pi r_r h_r + 2\pi r_r^2)\ x \tag{7}$$

Where r_r is the radius of the reaction chamber.

Thermal Insulation Thickness

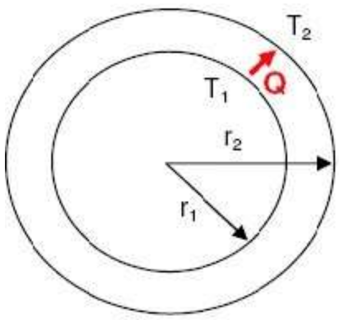

Figure 3: Schematic diagram, showing the cross section of the reactor housing

The thickness of the thermal insulation layer was calculated based on the properties of the lagging material to ensure effective minimization of heat loss. Considering figure 5, which shows the cross section of the reactor housing, r_1 and r_2 is the internal and external radius of the reactor housing respectively, $T_{r1}$and T_{r2} is the temperature within and the expected temperature outside the reactor housing, respectively. While Q is the quantity of heat supplied within the reactor housing. Therefore, to determine the insulation thickness, r_2 will be calculated using equation (8), since the internal radius of the reactor housing is known.

$$Q = \frac{(T_{r_1} - T_{r_2})}{In\left(\frac{r_2}{r_1}\right)/2\pi K h_{r_h}} \quad (8)$$

Where K the thermal conductivity of the lagging material, and h_{rh} is the height of the reactor housing. Hence the insulation thickness (X_L) was calculated using equation (9);

$$X_L = (r_2 - r_1) \quad (9)$$

Fabrication

The fabrication of the reactor was conducted in strict adherence to established fabrication standards. Initially, the acquired materials were accurately marked and cut to the specified shapes and dimensions using appropriate cutting equipment. Subsequently, holes were precisely drilled at predetermined locations in accordance with specified tolerances to ensure accurate assembly. The fabricated components were then joined through welding, employing suitable welding methods to achieve robust and defect-free joints. Following welding, surface finishing processes were undertaken, including grinding to remove excess weld deposits and smooth weld seams, edge filling to eliminate sharp edges and ensure uniformity, and sanding to remove rust, scale, and other surface impurities. To protect the components from corrosion and to enhance their aesthetic appeal, a corrosion-resistant spray paint coating was applied. Finally, the fabricated components were assembled using bolts and nuts in strict accordance with the production drawings, ensuring proper alignment and structural integrity of the reactor assembly.

Test and Evaluation

The hydrothermal carbonization reactor was tested using African Fan Palm Nut at different voltage levels (185V, 210V, and 220V) to evaluate its heating performance. The reactor was set to reach target temperatures of 180°C, 200°C, and 220°C, and the corresponding heating times were recorded. These conditions were based on work reported by Brilman et al (2017) Results showed that increasing voltage reduced the time required to attain the set temperatures, indicating improved heating efficiency. The evaluation confirmed a linear relationship between temperature and time, with faster heating rates observed at higher voltages as shown in figure 7.

RESULTS AND DISCUSSION

Graphics Design Result

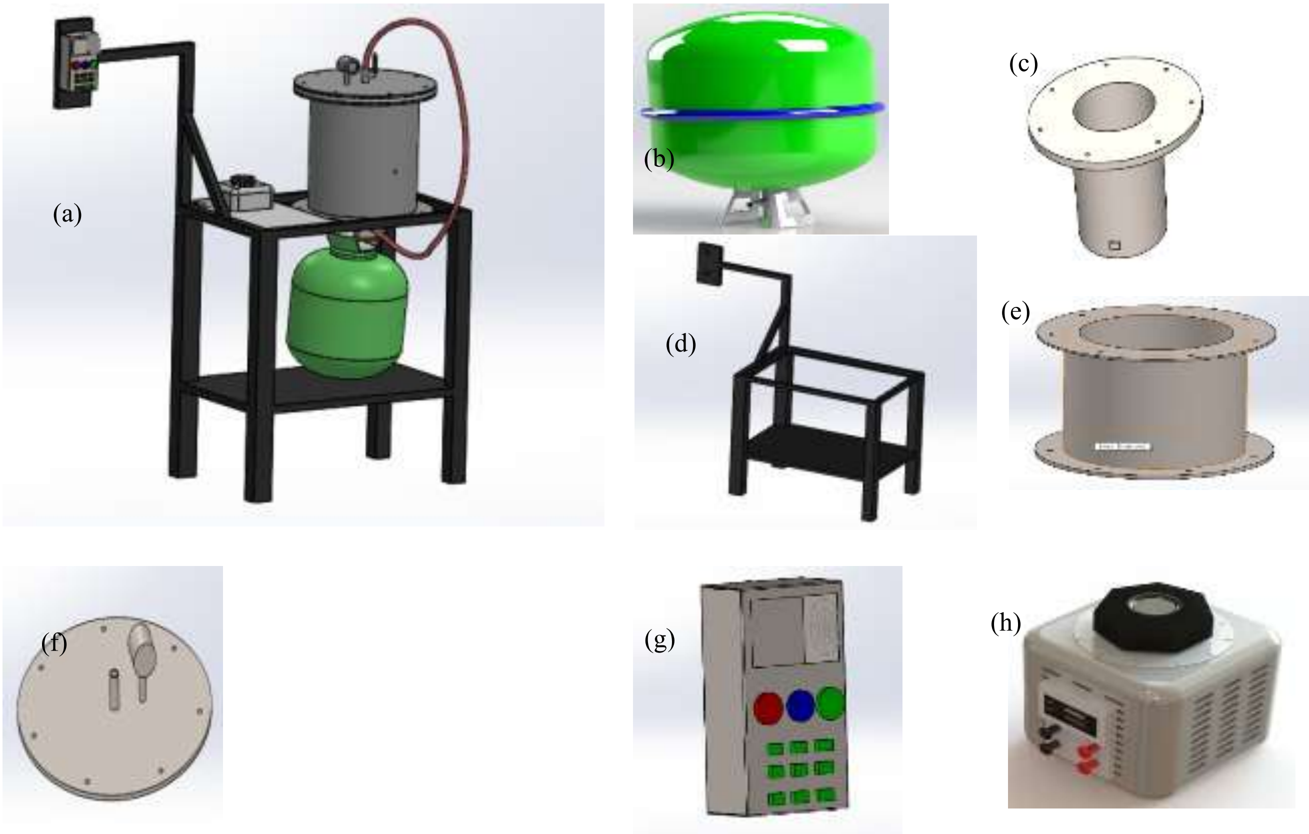

Figure 4: Graphics model of the designed reactor

The graphical models of the designed reactor and its components are presented in Figure 4. (a) Assembled reactor. (b) Gas tank, where the gaseous products are discharged (c) Reaction chamber, with an external heater wound around it to supply the necessary heat for the reaction. (d) Supporting frame, which provides the base for the reactor and its components. (e) Reactor housing, enclosing the reaction chamber. (f) Reaction chamber cover, equipped with a relief valve connected to the gas cylinder and a pressure gauge to monitor pressure during the reaction. (g) Control box housing all electrical components, including the thermocouple and magnetic contactor. (h) Voltage regulator responsible for controlling the heating rate.

Mathematical Design Results

Table 1: The reactor parameters obtain from the mathematical design

Reactor Parameter	Symbol	Quantity	Unit	Source
Volume of wet biomass	V_{wb}	0.0012	m3	Considered
Volume of reaction chamber	V_r	0.0016	m^3	Equation (1)
Diameter of the reaction chamber	d_r	0.102	m	Considered to allow for stirrer.
Height of the reaction chamber	h_r	0.2	m	Equation (2)
Maximum internal pressure	P_i	4	MPa	Considered, liquefaction Pressure range
External Pressure	P_o	0.101325	MPa	Atmospheric pressure
Hoop stress	σ_h	505	MPa	Aerospace Specification Metal Inc. (ASM)

Reactor Parameter	Symbol	Quantity	Unit	Source
Reaction chamber wall thickness	x	5	mm	Equation (3)
Volume of the reaction chamber material	V_{rm}	0.000402	m3	Equation (6)
Density of the reaction chamber wall material	ρrm	8000	Kg/m^3	Aerospace Specification Metal Inc. (ASM)
Mass of reaction chamber material	*mrm*	3.216	kg	Equation (5)
Specific heat capacity of stainless steel	*cp*	502.416	J/Kg-K	Aerospace Specification Metal Inc. (ASM)
Change in temperature between the desired and atmospheric temperature	ΔT	473	°C	Equation (5)
Time required to reach maximum temperature	*t*	10	mins	Considered
Heater capacity	*E*	2	KW	Equation (4)
Maximum desired temperature	*T1*	500	°C	Considered, liquefaction temperature range
Thermal conductivity of lagging material	*K*	0.48	Wm-1K-1	Mgbemena et al, (2019)
Height of reactor housing chamber	*rrh*	0.33	m	Considered to house the reaction chamber
Internal radius of the reactor housing	*r1*	0.102	m	Considered
External radius of the reactor housing	r_2	0.15	m	Equation (8)
Thermal insulation thickness	*XL*	0.1	m	Equation (9)

The table above (table 1) shows the result of the mathematical designed parameters for the modelled reactor. Some considered parameter was done for easy of fabrication and operation. Parameters such as thermal conductivity specific heat capacity and other parameters that describe the properties of some the materials used were obtained from available literature as reported in the table. While the rest of the other parameters was calculated using the quoted equations to enable the fabrication of functional and reliable reactor.

Thermal Distribution and Static Stress Simulation Result

Thermal distribution analysis of the reactor housing, as illustrated in Figure 5, was carried out to evaluate the effectiveness of the selected insulation. From the figure, it can be observed that the chosen insulation materials and thickness are sufficient to insulate the reactor housing effectively, thereby minimizing heat loss. Figure 6 presents the static stress simulation of the reaction chamber. This analysis is crucial to determine whether the selected wall thickness of the reaction chamber can adequately withstand the expected thermal and mechanical stresses, based on the material chosen for its construction. The simulation results indicate a maximum induced stress of 4.752×10^8 N/m² within the chamber, which is below the material's yield strength of 6.204×10^8 N/m², as shown in the Von Mises stress distribution bar in Figure 6. This confirms that the design meets structural integrity requirements and is suitable for the reactor's reaction chamber fabrication.

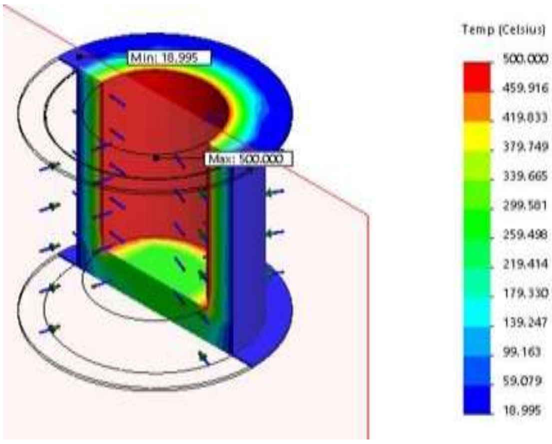

Figure 5: Simulated model showing thermal distribution along reactor housing walls

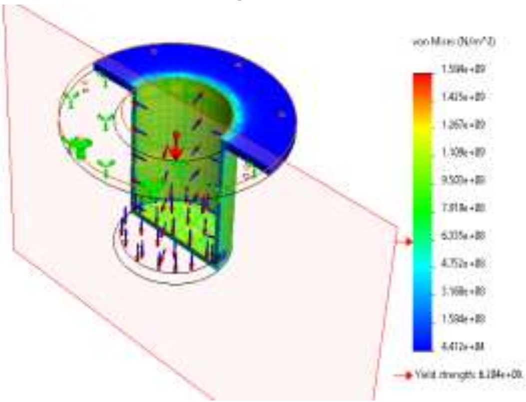

Figure 6: Static stress simulation analysis result of the reaction chamber

Developed Reactor and its Operation

The assembled hydrothermal liquefaction reactor is shown in Figure 9. It is operated by arranging the components as depicted. The reactant is placed inside the reaction chamber, which is then securely sealed using either bolts and nuts or a high-torque clamp. A high-temperature-resistant Teflon gasket is positioned between the reactor flange and the cover to prevent pressure leakage. The reactor is connected to the power supply via a voltage regulator. The voltage is adjusted to the desired setpoint to achieve the required heating rate. Before starting the reaction, ensure the pressure valve is completely closed; it should only be opened when pressure regulation is necessary.The desired reaction temperature is set using the thermocouple control, and the heater is then activated. The reaction proceeds until the predetermined reaction time elapses. Afterward, the reactor is turned off and allowed to cool before disassembly. It is important to ensure that all gaseous products are fully vented into the gas collection tank by opening the valve before loosening the clamp or unsealing the chamber.

Figure 6: The picture of the produced reactor

Calibration Result of the Reactor's Heating Rate

Table 2: Heating rate calibration at 185 V

S/N	Voltage (V)	Target temp (°C)	Time(mins)	Heating rate($^{\circ}C/_{min}$)
1	185	180	36	5.0
2	185	200	40	5.0
3	185	220	44	5.0

Table 3: Heating rate calibration at 210 V

S/N	Voltage (V)	Target temp (°C)	Time(mins)	Heating rate($^{\circ}C/_{min}$)
1	210	180	33	5.45
2	210	200	36	5.56
3	210	220	40	5.50

Table 4: Heating rate calibration at 220 V

S/N	Voltage (V)	Target temp (°C)	Time(mins)	Heating rate($^{\circ}C/_{min}$)
1	220	180	30	6.00
2	220	200	33	6.06
3	220	220	37	5.95

Table 5: Table of experimented voltages and the corresponding heating rate.

Voltage (V)	Average Heating Rate ($^{\circ}C/_{min}$)
185	$\frac{5.00+5.00+5.00}{3}$ = 5.00

210	$\frac{5.45+5.56+5.50}{3} = 5.50$
220	$\frac{6.00+6.06+5.96}{3} = 6.00$

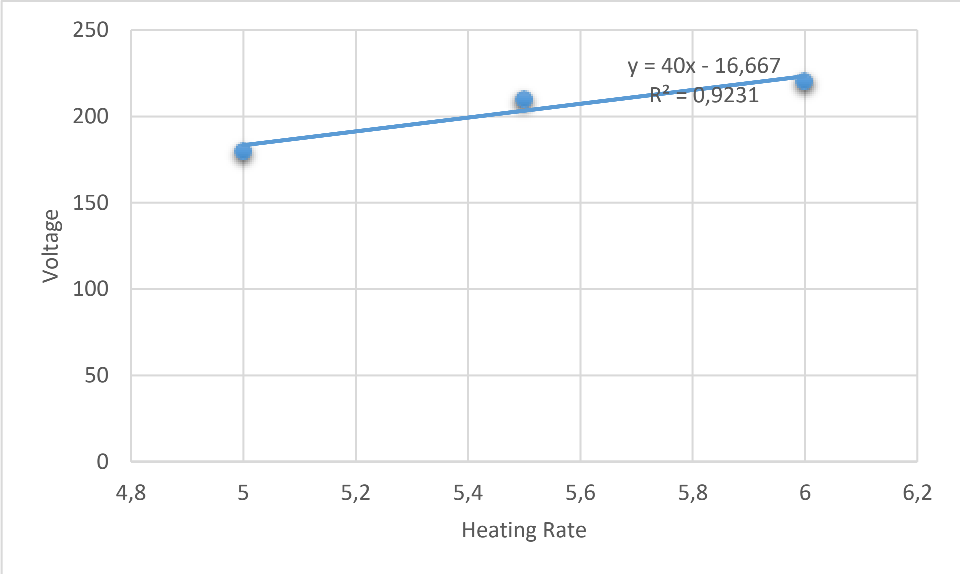

Fig 7: Graph of voltage against heating rate

The graph illustrates how various voltages levels affect the reactors heating rate. It reveals that as the voltage increases, the reactor heats up more quickly, following a linear trend.

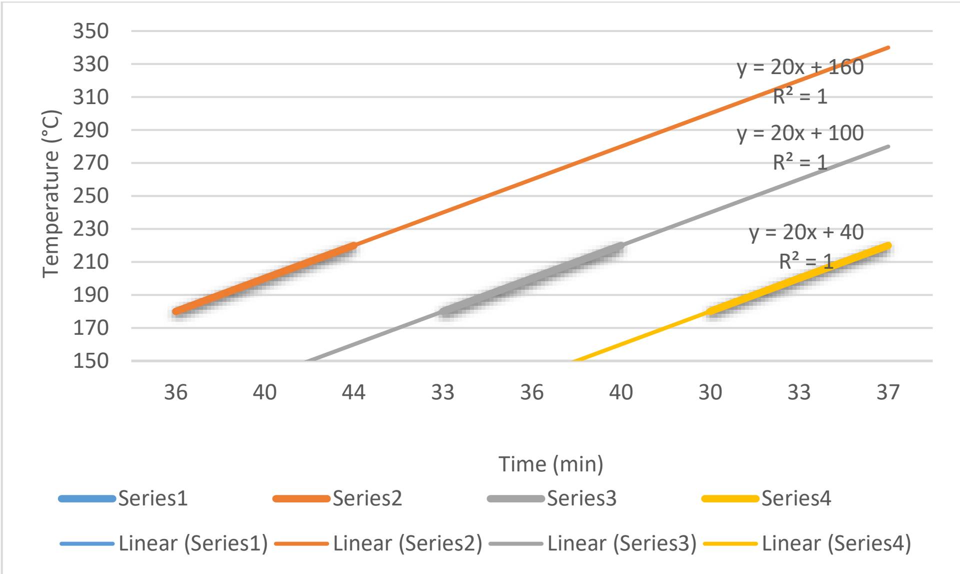

Fig 8: Graph of Temperature at different voltage against time

The graph illustrates how the temperature of the hydrothermal carbonization reactor increases over time under three different voltage levels: 185V, 210V, and 220V. Each voltage level exhibits a linear relationship between temperature and time, as indicated by the linear trend lines fitted to the data series.

CONCLUSIONS

The project successfully designed and developed a laboratory-scale hydrothermal carbonization reactor capable of converting biomass into hydrochar under controlled temperature and pressure. Solidworks (2020) was used in modelling and simulation of the HTC reactor to determine the stresses acting on the different component

The design meets critical performance criteria for HTC processes and demonstrates potential for further development, particularly in decentralized waste management and bioenergy applications. Although fabrication and operation presented technical challenges, they were overcome through careful material selection, safety planning, and iterative design improvements. Future work could include automation of the process, scale-up for industrial use, and comprehensive testing across a wider range of feedstocks to assess efficiency and product quality.

REFERENCES

1. Ho, T. T.-T., Nadeem, A., & Choe, K. (2024). A review of upscaling hydrothermal carbonization. Energies, 17(8), 1918. https://doi.org/10.3390/en17081918
2. Merzari, F., Lucian, M., Volpe, M., Andreottola, G., & Fiori, L. (2018). Hydrothermal carbonization of biomass: Design of a bench-scale reactor for evaluating the heat of reaction. Chemical Engineering Transactions, 65, 43–48. https://doi.org/10.3303/CET1865008
3. Obi, O. F., Olugbade, T. O., Orisaleye, J. I., & Pecenka, R. (2023). Solid biofuel production from biomass: Technologies, challenges, and opportunities for its commercial production in Nigeria. Energies, 16(24), 7966. https://doi.org/10.3390/en16247966
4. Reza, M. T., Andert, J., Herklotz, B., Busch, D., & et al. (2014). Review article: Hydrothermal carbonization of biomass for energy and crop production. Applied Bioenergy, 1(1), 11–29. https://doi.org/10.2478/apbi-2014-0001
5. Umar, Y., Yakubu, R. O., Abdulazeez, A. A., & Ijeoma, M. W. (2024). Exploring Nigeria's waste-to-energy potential: A sustainable solution for electricity generation. Clean Energy, 8(6), 82–95. https://doi.org/10.1093/ce/zkae080
6. Wang, T., Zhai, Y., Zhu, Y., Li, C., & Zeng, G. (2018). A review of the hydrothermal carbonization of biomass waste for hydrochar formation: Process conditions, fundamentals, and physicochemical properties. Renewable and Sustainable Energy Reviews, 90, 223–247. https://doi.org/10.1016/j.rser.2018.03.071
7. Berge, N. D., Ro, K. S., Mao, J., Flora, J. R., Chappell, M. A., & Bae, S. (2011). Hydrothermal carbonization of municipal waste streams. Environmental Science & Technology, 45(13), 5696–5703. https://doi.org/10.1021/es2004528
8. Funke, A., & Ziegler, F. (2010). Hydrothermal carbonization of biomass: A summary and discussion of chemical mechanisms for process engineering. Biofuels, Bioproducts and Biorefining, 4(2), 160–177. https://doi.org/10.1002/bbb.198
9. He, C., Giannis, A., & Wang, J. Y. (2018). Conversion of sewage sludge to clean solid fuel using hydrothermal carbonization: Hydrochar fuel characteristics and combustion behavior. Applied Energy, 111, 257–266. https://doi.org/10.1016/j.apenergy.2013.04.084
10. Kambo, H. S., & Dutta, A. (2015). A comparative review of biochar and hydrochar in terms of production, physico-chemical properties and applications. Renewable and Sustainable Energy Reviews, 45, 359–378. https://doi.org/10.1016/j.rser.2015.01.050
11. Kruse, A., Funke, A., & Titirici, M. M. (2013). Hydrothermal conversion of biomass to fuels and energetic materials. Current Opinion in Chemical Biology, 17(3), 515–521. https://doi.org/10.1016/j.cbpa.2013.05.004
12. Libra, J. A., Ro, K. S., Kammann, C., Funke, A., Berge, N. D., Neubauer, Y., Titirici, M. M., Fühner, C., Bens, O., Kern, J., & Emmerich, K. H. (2011). Hydrothermal carbonization of

biomass residuals: A comparative review of the chemistry, processes and applications of wet and dry pyrolysis. Biofuels, 2(1), 71–106. https://doi.org/10.4155/bfs.10.81

13. Nwoke, G. O., Abam, F. I., & Mbohwa, C. (2021). Hydrothermal carbonization of biomass for energy generation in Sub-Saharan Africa: Potential, challenges, and prospects. Energy Reports, 7, 7743–7753. https://doi.org/10.1016/j.egyr.2021.01.036
14. Obi, O. F., Ugwuishiwu, B. O., & Ekoh, D. A. (2022). Thermal and fuel characteristics of hydrochar produced from palm kernel shell using hydrothermal carbonization. Renewable Energy Focus, 40, 1–10. https://doi.org/10.1016/j.ref.2022.04.008
15. Pandey, A., Ojha, A., & Kumar, R. (2017). Design and development of semi-continuous hydrothermal carbonization reactor for energy recovery from urban food waste. Renewable Energy, 113, 1240–1247. https://doi.org/10.1016/j.renene.2017.06.069
16. Reza, M. T., Rottler, E., Herklotz, L., Wirth, B., & Lehmann, F. (2014). Influence of hydrothermal carbonization on fuel properties of sewage sludge. Fuel, 140, 107–115. https://doi.org/10.1016/j.fuel.2014.09.032
17. Sevilla, M., & Fuertes, A. B. (2009). The production of carbon materials by hydrothermal carbonization of cellulose. Carbon, 47(9), 2281–2289. https://doi.org/10.1016/j.carbon.2009.04.026
18. Shen, Y., Linville, J. L., Urgun-Demirtas, M., Mintz, M. M., & Snyder, S. W. (2015). Heating up the biorefinery? Energetic and environmental challenges in scaling up hydrothermal carbonization of organic waste. Journal of Cleaner Production, 93, 318–326. https://doi.org/10.1016/j.jclepro.2015.01.009
19. Wang, T., Zhai, Y., Zhu, Y., Li, C., Zeng, G., & Liu, Y. (2018). A review of the hydrothermal carbonization of biomass waste for hydrochar formation: Process conditions, fundamentals, and physicochemical properties. Renewable and Sustainable Energy Reviews, 90, 223–247. https://doi.org/10.1016/j.rser.2018.03.071
20. Yahya, A., Johari, A., & Hashim, H. (2018). Hydrothermal carbonization of biomass for energy and resources recovery: A review. Renewable and Sustainable Energy Reviews, 90, 583–604. https://doi.org/10.1016/j.rser.2018.03.072
21. Zhang, L., Xu, C., & Champagne, P. (2019). Overview of recent advances in thermochemical conversion of biomass into biofuels. Bioresource Technology, 183, 1–15. https://doi.org/10.1016/j.biortech.2013.06.091
22. Ezenwa, O. N., Mgbemena, C. O., & Emagbeterre, E. (2023). Design and construction of a continuous stirring hydrothermal liquefaction batch reactor. Tuijin Jishu/Journal of Propulsion Technology, 44(3), 2021–2031. https://doi.org/10.52783/tjjpt.v44.i3.635